Organic & Biomolecular Chemistry

Dynamic Article Links

Cite this: *Org. Biomol. Chem.*, 2011, **9**, 5554

www.rsc.org/obc

**PAPER**

# Molecular dynamics simulations of the *Salmonella typhi* Vi antigenic polysaccharide and effects of the introduction of a zwitterionic motif

**Laura Legnani,[a] Federica Compostella,[b] Giovanni Grazioso,[c] Franca Marinone Albini[a] and Lucio Toma*[a]**

***Received 18th April 2011, Accepted 13th May 2011***
**DOI: 10.1039/c1ob05617d**

A series of hexasaccharides corresponding to the Vi capsular polysaccharide, a polymer of α-(1→4)-galacturonic acid, and analogs containing a zwitterionic motif with various degrees of acetylation at positions 3 have been modeled. When submitted to molecular dynamics simulations in a water box, all the structures visited only two quite restricted regions of the $\phi/\psi$ conformational space both corresponding to extended geometries without any tendency towards supercoiling. The most stable conformation showed a clockwise helix arrangement of substituents on the molecular surface whereas the opposite arrangement was observed for the other conformation. The flexibility of the system and the hydrophobic character of the molecular surface are modulated by the 3-*O*-acetyl groups that confer rigidity to the system. In the zwitterionic analogs, the introduction of positive charges in the place of the acetamido groups alters the hydrophobicity that can be regained by methylation of the amino groups. The needed molecular flexibility can be obtained by the complete deacetylation at positions 3.



## Introduction

The capsular polysaccharides of several bacteria are important virulence factors and induction of antibodies specific to them confers protection against bacterial infection. In fact, they have been extensively studied for their potential use as vaccines.[1]

Vi antigen **I** (Chart 1) is a capsular polysaccharide present in several members of the family of *Enterobacteriaceae*. It is a polymer of α-(1→4)-galacturonic acid with an *N*-acetyl at position 2 and variable *O*-acetylation at C-3,[2] and it is associated with the virulence of *Salmonella typhi*, a bacterial pathogen that causes typhoid fever in humans. Currently it is one of the two internationally licensed vaccines available for protection against typhoid fever.[3]

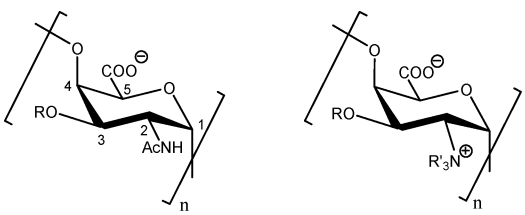


**I**: R = H, Ac

**II**: R = H, Ac; R' = H
**III**: R = H, Ac; R' = $CH_3$

**Chart 1**

Studies performed on native Vi antigen showed[4] that its immunogenicity is closely related to the degree of 3-*O*-acetylation; indeed, the 3-*O* peracetylated or partially acetylated polysaccharides are immunogenic while the deacetylated one is not. In contrast, carboxyl groups show a relatively slight influence. In order to rationalize these biological results the same authors, using CPK space-filling models, observed that the bulky *O*- and *N*-acetyl groups dominate the surface of the Vi polysaccharide and could shield the carboxyl groups from interaction with other molecules. As a consequence, the effects of the removal of the acetyl groups on the overall 3D conformation of the polymer, and therefore on the possible exposure of the anionic groups, is an important issue still to be clarified due to the undoubted consequences of this chemical modification on the biological activity.

The main flaws associated with pure polysaccharide (PS) vaccines are their poor immunogenicity and short-term, incomplete protection. In fact, PSs are T-independent antigens. As a consequence, no booster effect is observed by repeated injections, indicating the lack of immunological memory. In addition, these vaccines are not effective in young children. These limitations have been sometimes overcome with the development of conjugated vaccines,[5] but the obtainment of better formulations and the comprehension/control of the immunological events under analysis are urgently needed.

It is known that two polysaccharide components of *Bacteroides fragilis*, the PS A1 and PS A2 antigens, are able to activate T cells.[6] The primary structure of these glycoantigens consists of a tetra- and a pentasaccharide repeating unit, respectively, possessing constituent sugars with free amino and carboxyl groups. Their

[a]*Dipartimento di Chimica, Università di Pavia, Via Taramelli 12, 27100 Pavia, Italy. E-mail: lucio.toma@unipv.it; Fax: +39-0382-987323; Tel: +39-0382-987843*
[b]*Dipartimento di Chimica, Biochimica e Biotecnologie per la Medicina, Università di Milano, Via Saldini 50, 20133 Milano, Italy*
[c]*Dipartimento di Scienze Farmaceutiche "Pietro Pratesi", Università degli Studi di Milano, via L. Mangiagalli 25, 20133 Milano, Italy*

immunogenic activity is dependent on the presence of the zwitterionic motif and on the molecular mass.[6] Elimination of either of the charged groups results in a lack of *in vivo* T-cell activation. This feature is common to other T-cell activating glycoantigens, which naturally contain both positive and negative charges, such as the polysaccharides (PS) from *Streptococcus pneumoniae* type 1 (Sp1) and *Staphylococcus aureus*.[7] The immunogenic activity of structurally different zwitterionic PSs is supposed to be closely linked with their three-dimensional conformation and overall spatial charge organization.[6,7] In fact, a combination of NMR spectroscopy and molecular mechanics and dynamics calculations led to the determination that PS A2 and Sp1 assume a helical conformation where all charges are exposed on the outer surface of the polymer in a regularly spaced pattern. So, distinct zwitterionic PSs may assume similar 3D structures to define a common scaffold for the presentation of charges. However, it remains unclear whether the zwitterionic charge motif is solely responsible for binding (electrostatically) or is needed for a particular 3D conformation that facilitates the binding process.[8]

The observation that the presence of a zwitterionic motif in bacterial PSs confers the ability to activate T cells suggests the possibility to introduce T-cell activating properties into a polysaccharide by chemical modification. Actually, it has been shown that the conversion of the Vi antigen into a structure in which the *N*-acetyl group is chemically cleaved, presenting both positive and negative charges, is able to confer immunity in a T-cell dependent manner.[6a]

Being involved in a project aimed at the design, preparation, and test of structural analogs of the Vi antigen endowed with T-cell dependent immunogenic properties, a preliminary detailed investigation of the conformational properties of native Vi PSs, and of the effects of possible chemical modifications on these properties, is needed. Thus, we used a computational approach, based on updated theoretical tools, to determine the geometrical properties of the Vi antigen **I** as well as of its derivative **II** (Chart 1), in which the *N*-acetyl group has been cleaved. In both the cases structures with a variable degree of acetylation at position 3 were considered. Finally, the trimethylammonium derivative **III** (Chart 1) was considered to assess the effects of the shielding of the positive charge and of the increase of the steric bulk on the conformational properties of the compounds. Calculations were performed on hexasaccharide fragments of polysaccharides **I–III** (compounds **1–3**, Chart 2), that seem to be long enough to mimic, in relatively small molecules, their overall conformational properties.

## Results and discussion

Preliminary investigations on the conformational preferences at the GalANAc-α(1→4)-GalANAc glycosidic linkage through molecular dynamics simulations showed only two accessible regions of the $\phi/\psi$ map characterized, respectively, by values of $\varphi$ and $\psi$ both negative (**C1** conformation, $\phi_{avg} \approx -80°$, $\psi_{avg} \approx -40°$) and by values of $\phi$ prevalently positive and $\psi$ positive (**C2** conformation, $\phi_{avg} \approx 20°$, $\psi_{avg} \approx 40°$). In Fig. 1 a typical $\phi/\psi$ scatter plot is reported together with the 3D-plots of **C1** and **C2** significant conformations.

Then, we performed MD simulations on the hexasaccharide substructure of Vi antigen, *O*-methylated at the reducing end and at position 4 of the non-reducing end, fully acetylated at position 3 of each residue (**1a**). The simulations were carried out for 5 ns with the SANDER module of the AMBER 10 package[9] and using explicit water as solvent. They were repeated two times, choosing

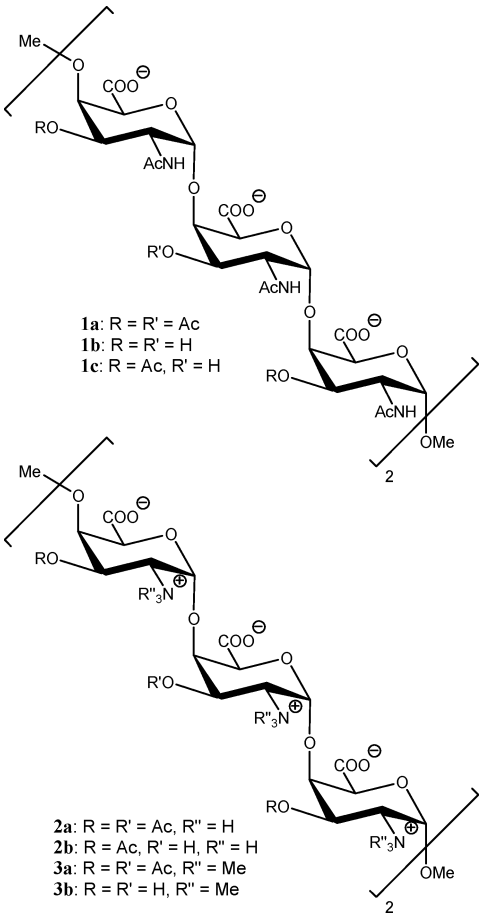


**Chart 2**

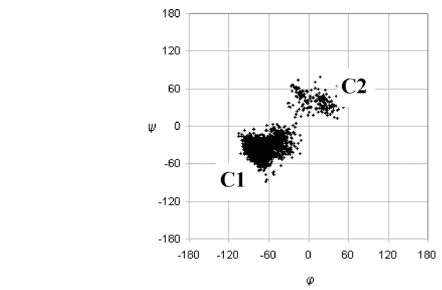


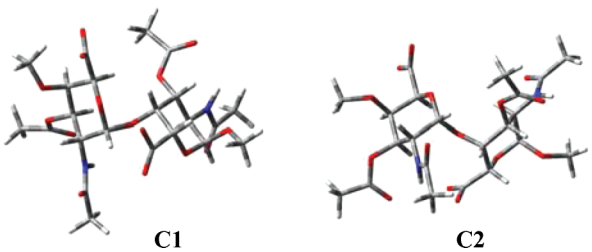


**Fig. 1** $\phi/\psi$ scatter plot of the populated conformations at the glycosidic linkage of the disaccharide GalANAc-α(1→4)-GalANAc from molecular dynamics simulations and three-dimensional plots of its **C1** and **C2** conformations.

two different starting geometries characterized by having the five inter-residue glycosidic linkages all in the **C1** geometry or all in the **C2** geometry. The trajectories of the $\phi$ and $\psi$ torsional angles were analyzed and in every case the same behavior was found. **C2** → **C1** transitions at most of the glycosidic bonds were observed, whereas the reverse transition was seldom observed suggesting **C1** as the most stable conformation. Fig. 2 shows, as an example, the trajectories of the $\phi_1$ and $\psi_1$ torsional angles, that are relative to the non-reducing end of the molecule, as well as the corresponding scatter plot of the populated conformations. Moreover, in order to describe the overall behavior in a unifying picture, the cumulative $\phi/\psi$ scatter plot deriving from a superimposition of the data from all the five glycosidic bonds in the two MD simulations is also reported (Fig. 3). It shows an almost complete similarity with that depicted in Fig. 2. The averaged $\phi$ and $\psi$ in the two **C1** and **C2** regions were determined with values of $\phi_{avg} = -71°$, $\psi_{avg} = -37°$ and $\phi_{avg} = 17°$, $\psi_{avg} = 35°$, respectively.

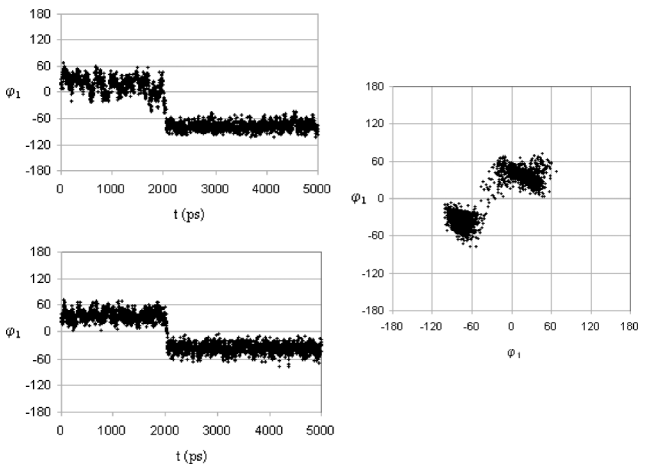


**Fig. 2** History of $\phi_1$ and $\psi_1$ in the MD simulation starting from conformation **C2** of hexasaccharide **1a** and the corresponding $\phi_1/\psi_1$ scatter plot.

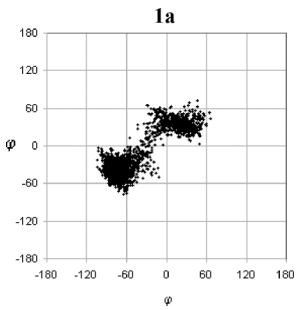


**Fig. 3** Cumulative $\phi/\psi$ scatter plot from the MD simulations on hexasaccharide **1a**.

The 3D plots of the **C1** and **C2** conformations of compound **1a**, presenting all their $\phi$ and $\psi$ torsional angles in the above reported averaged values are depicted in Fig. 4 using both a side and an axial view. The hexasaccharide assumes an extended geometry either in the **C1** or in the **C2** conformation and a quite similar distance between the anomeric oxygen at the reducing end and oxygen at C4 at the non-reducing end (25.8 and 26.3 Å, respectively).

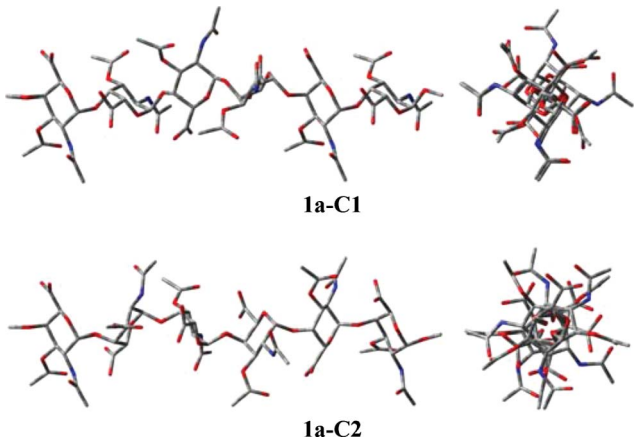


**Fig. 4** 3D-plots of the averaged **C1** and **C2** conformations of hexasaccharide **1a**: side and axial view (the hydrogen atoms are omitted for clarity).

In the mentioned study on the relationship between structure and immunological properties of Vi,[4] it was proposed that the bulky non-polar *O*-acetyl groups protrude in rows on both sides, impart rigidity to the structure and make up most of the surface, and that the carboxyl groups are less exposed and partially shielded by the *O*-acetyls. An alternating array of the substituents on the molecular surface was assumed, that corresponds to a rotation by 180° between two adjacent residues. These features are similar but not exactly the same as those found in conformations **C1** and **C2** obtained from the MD simulations. Actually, the 3D-plots of conformation **C1** in Fig. 4 show a helical arrangement of the substituents (Fig. 4 and 5); in fact, a clockwise rotation around the molecular axis by 90° of each residue with respect the preceding one is observed. Moreover, the carboxyl groups are exposed on the molecular surface. Also, conformation **C2** shows the substituents in a helical arrangement; however, in this case a counter-clockwise rotation by –138° between two adjacent residues is observed. Conformation **C1** is also characterized by a notable H–H inter-residue short distance between the hydrogen atom at C-5 of each residue and the hydrogen atom at C-4 of

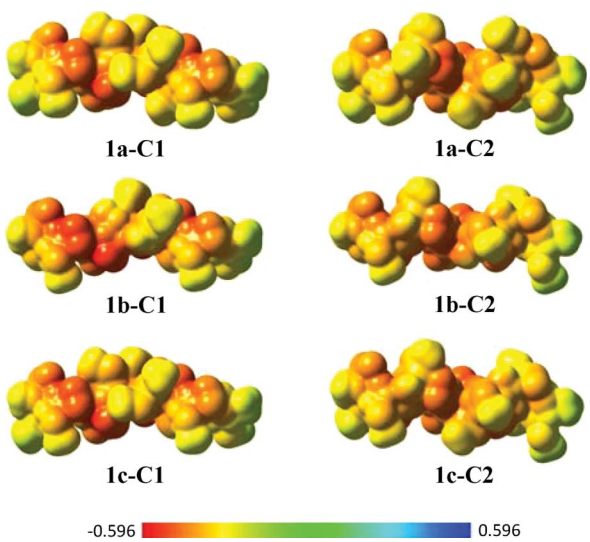


**Fig. 5** Electrostatic surface representation of the **C1** and **C2** conformations of hexasaccharides **1a–c**.

the adjacent residue ($d_{H5'\text{-}H4}$ = 2.3 Å), even shorter than the inter-glycosidic distance between the same hydrogen atom at C-4 and the adjacent anomeric hydrogen atom ($d_{H1'\text{-}H4}$ = 3.1 Å). Quite different distances are observed in conformation **C2** ($d_{H5'\text{-}H4}$ = 4.5 Å, $d_{H1'\text{-}H4}$ = 2.5 Å) where the hydrogen atom at C-5 becomes closer to the hydrogen atom at C-2 of the adjacent residue ($d_{H5'\text{-}H2}$ = 3.1 Å).

Then, our attention was focused on the 3-*O*-deacetylated and the partially deacetylated Vi analogs by submitting the hexasaccharides **1b** and **1c** to modeling studies. In the latter structure two of the six residues, namely the second and the fifth ones, present an unprotected hydroxyl group at C-3. The MD simulations were carried out with the same approach already described for **1a** and a similar data analysis was performed. The same two allowed conformations, **C1** and **C2**, were observed, but in these two cases a higher conformational flexibility could be observed. In fact, the trajectories of the $\phi$ and $\psi$ torsional angles showed a higher frequency of **C2** → **C1** transitions, in particular in the case of **1b**, where some reverse transitions were also observed. The cumulative $\phi/\psi$ scatter plot from MD simulations on **1b** and **1c**, deriving from a superimposition of the data from all the five glycosidic bonds are superimposable onto Fig. 3, indicating a negligible effect of 3-*O*-acetylation on the definition of the accessible regions of the conformational space. However, some effects on the molecular size (a smaller section) and on the polar/hydrophobic character of the surface could be observed (Fig. 5). Values of averaged $\phi$ and $\psi$ very similar to those observed for compound **1a** were determined (**1b**: **C1** conformation, $\phi_{avg} = -72°$, $\psi_{avg} = -41°$, **C2** conformation, $\phi_{avg} = 13°$, $\psi_{avg} = 35°$; **1c**: **C1** conformation, $\phi_{avg} = -71°$, $\psi_{avg} = -40°$, **C2** conformation, $\phi_{avg} = 16°$, $\psi_{avg} = 35°$), thus producing analogous values of notable inter-residue distances.

It is well known that the complete reduction of the *O*-acetyl content results in a polysaccharide that fails to elicit antibodies which are reactive with the native Vi.[4] As the accessible geometries of **1b** remain the same as those of **1a**, though in a molecule endowed with much more flexibility, this total loss of immunogenicity could be ascribed to a specific influence of the 3-*O*-acetyl groups that provide a bulky and nonpolar surface to Vi. Instead, the immunological studies on the partially 3-*O*-deacetylated Vi showed that the corresponding preparations elicited antibody levels equal to or greater than those for the native polymer.[4] The increased immunogenicity could be due to the increased flexibility of **1c** with respect to **1a** combined with the presence of a percentage of 3-*O*-acetylated positions sufficient to provide the necessary hydrophobic character of the molecular surface.

As already mentioned, the chemical cleavage of the *N*-acetyl groups of Vi by treatment with alkali results in a structure able to confer immunity in a T-cell dependent manner.[6a] Thus, the modeling study was extended to the hexasaccharide analogs **2** in which the nitrogen atoms are in the form of ammonium groups and a zwitterionic motif is introduced in the molecule. Also in this case the effects of 3-*O*-acetylation were considered, through the study of the fully and the partially acetylated structures, **2a** and **2b**, respectively.

Fig. 6 shows the cumulative $\phi/\psi$ scatter plots from the MD simulations on **2a** and **2b**, which are very similar to those of **1a** and **1c**. The **C1** region is quite superimposable with that of Fig. 3, whereas the **C2** region is shifted to lower values of $\phi$, as can also be seen from the corresponding values of averaged $\phi$ and $\psi$ (**2a**: **C1** conformation, $\phi_{avg} = -60°$, $\psi_{avg} = -36°$, **C2** conformation, $\phi_{avg} = -25°$, $\psi_{avg} = 24°$; **2b**: **C1** conformation, $\phi_{avg} = -61°$, $\psi_{avg} = -37°$, **C2** conformation, $\phi_{avg} = -24°$, $\psi_{avg} = 23°$). In Fig. 7 the 3D-plots of the averaged **C1** and **C2** conformations of compound **2a** are depicted, whereas Fig. 8 reports the electrostatic surface representations. The notable H–H inter-residue short distances that characterize conformation **C1** are similar to those observed in **1a** ($d_{H5'\text{-}H4}$ = 2.5 Å; $d_{H1'\text{-}H4}$ = 3.0 Å). Conversely, significant differences are observed in conformation **C2** ($d_{H5'\text{-}H4}$ = 4.1 Å, $d_{H1'\text{-}H4}$ = 2.3 Å; $d_{H5'\text{-}H2}$ = 2.1 Å). The observed plots and data of **2b** are practically identical to those of **2a** indicating that also in this case the accessible geometries remain the same and only flexibility increases.

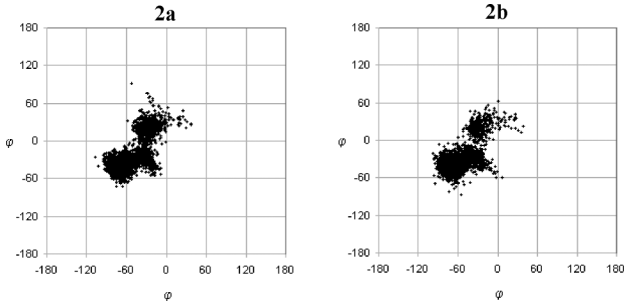


**Fig. 6** Cumulative $\phi/\psi$ scatter plots from the MD simulations on hexasaccharides **2a** and **2b**.

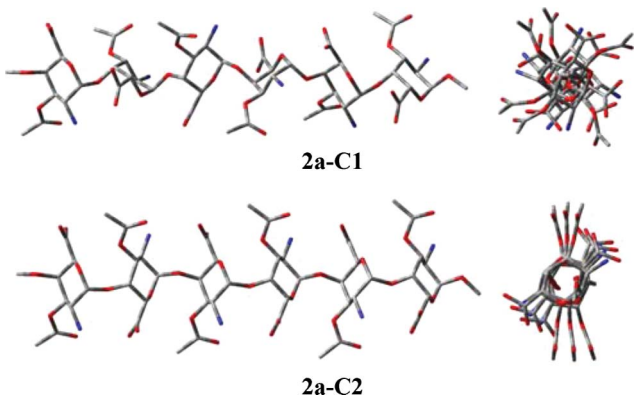


**Fig. 7** 3D-plots of the averaged **C1** and **C2** conformations of hexasaccharide **2a**: side and axial view (the hydrogen atoms are omitted for clarity).

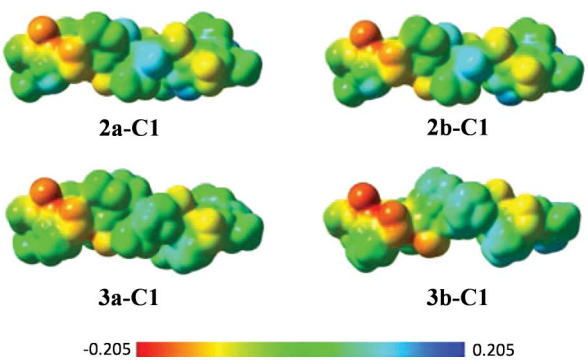


**Fig. 8** Electrostatic surface representation of the **C1** conformations of hexasaccharides **2** and **3**.

The overall shape of compounds **2a** and **2b** is quite different from that suggested for PS A2 and Sp1 zwitterionic polysaccharides.

Both these PSs have been described[6,7] as right-handed helices with a pitch of 20 Å characterized by regular series of grooves. The positive and negative charges exposed on the surface of the molecules, in PS A2 alternate along the sides of the chain with an approximate distance of 10 Å and in Sp1 are at distances of 7.3–7.4 Å. Also in conformations **C1** of **2a** and **2b** the positive and negative charges are on the molecular surface but no tendency towards supercoiling was observed. Distances of 4.2 or 7.3 Å between adjacent couples of opposite charges were determined, the longer one corresponding to that found in Sp1. This diversity in the shape and charge organization could help to clarify whether a particular conformation is needed for inducing activation of T-cells or the zwitterionic charge motif is solely responsible for the binding process.[8]

Finally, an analog of Vi in which a trimethylammonium group replaces the ammonium group of **2** (or the amido group of **1**) was modeled. Thus, the hexasaccharide substructures **3**, in which the positive charges are shielded by the presence of three methyl groups, were modeled through the study of the fully 3-*O*-acetylated structure **3a** and the fully deacetylated structure **3b**.

Also in this case 3-*O*-acetylation does not influence the conformational preferences at the glycosidic linkages as can be seen from the cumulative $\phi/\psi$ scatter plots in Fig. 9. Only flexibility differentiates **3b** from **3a**; whereas **3a** has a very limited tendency to transitions between the **C1** and **C2** conformations, in the MD simulations starting either from conformation **C1** or from conformation **C2**, compound **3b** showed the same degree of flexibility usually found in the partially acetylated structures **1c** and **2b**. The **C1** region maintains the usual shape whereas the **C2** region is more extended along the $\psi$ axis. This corresponds to values of averaged $\phi$ and $\psi$ still similar to the previous cases for conformation **C1** (**3a**: $\phi_{avg} = -61°$, $\psi_{avg} = -40°$; **3b**: $\phi_{avg} = -62°$, $\psi_{avg} = -39°$) and somewhat different to conformation **C2** (**3a**: $\phi_{avg} = -26°$, $\psi_{avg} = 57°$; **3b**: $\phi_{avg} = -25°$, $\psi_{avg} = 58°$). In Fig. 10, the 3D plots of the averaged **C1** and **C2** conformations of compound **3a** are depicted, whereas in Fig. 8 are the electrostatic surfaces. Also for **3a** and **3b** the H–H inter-residue short distances of conformation **C1** are similar to those usually observed (**3a**: $d_{H5'\text{-}H4} = 2.5$ Å; $d_{H1'\text{-}H4} = 3.1$ Å, **3b**: $d_{H5'\text{-}H4} = 2.4$ Å; $d_{H1'\text{-}H4} = 3.1$ Å) whereas conformation **C2** resembles more closely the corresponding geometry observed in compounds **2** (**3a**: $d_{H5'\text{-}H4} = 4.4$ Å, $d_{H1'\text{-}H4} = 2.5$ Å; $d_{H5'\text{-}H2} = 2.1$ Å, **3b**: $d_{H5'\text{-}H4} = 4.4$ Å, $d_{H1'\text{-}H4} = 2.6$ Å; $d_{H5'\text{-}H2} = 2.1$ Å). Distances of 4.6 or 7.5 Å between adjacent couples of opposite charges were determined in conformation **C1** of both **3a** and **3b**.

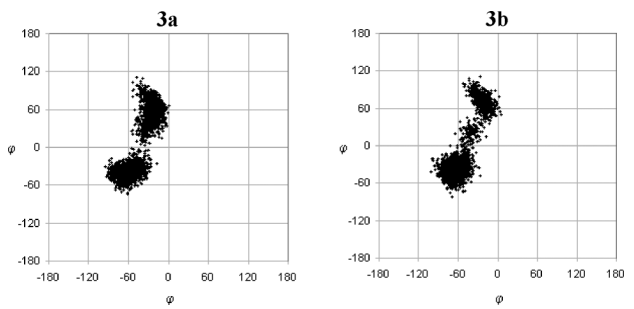


**Fig. 9** Cumulative $\phi/\psi$ scatter plots from the MD simulations on hexasaccharide **3a** and **3b**.

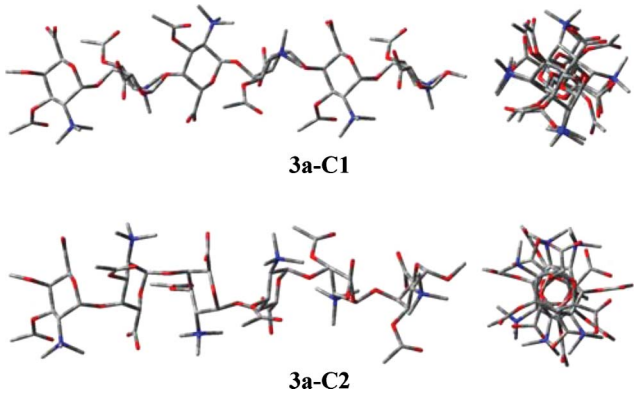


**Fig. 10** 3D-plots of the averaged **C1** and **C2** conformations of hexasaccharide **3a**: side and axial view (the hydrogen atoms are omitted for clarity).

## Conclusions

A series of hexasaccharide fragments corresponding to the Vi capsular polysaccharide and to analogs containing a zwitterionic motif, all with various degrees of acetylation at positions 3, have been modeled in order to determine the conformational preferences of the anionic saccharide Vi and the effects of the additional positive charge at positions 2.

When submitted to molecular dynamics simulations in a water box, all hexasaccharides **1–3** visited only two quite restricted regions of the $\phi/\psi$ conformational space exemplified by the **C1** and **C2** conformations. They correspond to extended geometries with a distance between the two ends of the molecules of about 25–26 Å and no observed tendency towards supercoiling. However, the rotated orientation around the molecular axis of each residue with respect to the preceding one leads to a helix arrangement of substituents on the molecular surface both in conformation **C1** and **C2**. While **C1** shows in all the modeled structures a clockwise rotation by about 90°, in **C2** the rotation occurs in the opposite direction for **1** (about −140°) and **3** (about −155°), whereas for **2** an almost regular alternating array is observed (about 180°).

The stability of conformation **C1** was found in all the cases to be higher than that of **C2** and the ease of transitions between the two geometries was largely influenced by the presence of the acetyl groups at positions 3. The 3-acetate groups confer rigidity to the system, so that some content of free hydroxyl groups at positions 3, such as those present in **1c**, seems necessary to give flexibility to the molecules. The hydrophobic properties of the molecular surface are guaranteed by the acetate groups still remaining at positions 3 as well as by the acetamido groups at positions 2.

The introduction of positive charges through exposition of the amino groups at position 2 (compounds **2**) causes a decrease of the hydrophobic character of the molecular surface that can be regained by methylation of nitrogens transformed into trimethylammonium groups (compounds **3**). The bulkiness of these groups makes structure **3a** excessively rigid and only the fully 3-*O*-deacylated structure **3b** acquires the needed molecular flexibility. In the latter compound, however, the hydrophobic character of the molecular surface is guaranteed by the trimethylammonium groups so that the 3-*O*-acetates do not seem necessary to control the molecular properties. Thus, compound **3b** seems a good candidate for mimicking the properties of natural Vi antigen

 

polysaccharide in a structure that, owing to its zwitterionic nature, could be endowed with the ability of activating T-cells.

## Experimental

### Computational methods

All MD simulations were performed with the SANDER module of the AMBER 10 package[9] along with the general amber force field (gaff)[10] and RESP atomic charges.[11] The TIP3P model[12] was employed to explicitly represent water molecules. The oligosaccharides were immersed in a box containing about 1000 water molecules and, in the case of Vi, $Na^+$ counterions were added to maintain neutrality on the systems. At first, the energy of the water molecules was minimized, keeping the atoms of the oligosaccharides frozen. Then, a minimization of the whole system was performed by setting a convergence criterion on the gradient of $10^{-4}$ kcal $mol^{-1}$ $Å^{-1}$. Prior to starting the MD simulations, the system was equilibrated for 40 ps at 300 K in isocore conditions (NVT). Subsequently, 5 ns of MD simulations in isothermal-isobaric ensemble were carried out at 300 K with a 2 fs time-step (NPT). In the production runs, the systems were performed in periodic boundary conditions. Van der Waals and short-range electrostatic interactions were estimated within an 8 Å cutoff. The SHAKE algorithm[13] was applied to all bonds involving hydrogen atoms. VMD 1.8.7 was used for molecular visualization and for animating trajectory data.[14] Trajectory analyses were carried out on the glycosidic angles defined as $\phi$: H1′–C1′–O–C4, $\psi$: C1′–O–C4–H4. All the trajectories were carefully inspected and ring conformations checked. The correct $^4C_1$ conformation was the only one populated in all the monosaccharide residues confirming that the gaff force field, despite not being designed for carbohydrates, can properly model ring conformations.

## Acknowledgements

The Italian Ministry of University and Research (PRIN 2008 grant, prot. 2008CZ3NP3, Modeling and synthetic studies of antigenic bacterial polysaccharides and their zwitterionic analogues) and the Universities of Pavia (FAR grant) and Milan (PUR grant) are gratefully acknowledged for financial support. CILEA (Milan) is acknowledged for generous allocations of computer time.

## Notes and references

1 A. Gonzalez-Fernandez, J. Faro and C. Fernandez, *Vaccine*, 2008, **26**, 292–300.
2 (*a*) K. Heyns and G. Kiessling, *Carbohydr. Res.*, 1967, **3**, 340–353; (*b*) S. C. Szu and S. Bystricky, *Methods Enzymol.*, 2003, **363**, 552–567.
3 (*a*) X. L. Zhang, V. T. Jeza and Q. Pan, *Cell. Mol. Immunol.*, 2008, **5**, 91–97; (*b*) D. De Roeck, L. Jodar and J. N. Clemens, *N. Engl. J. Med.*, 2007, **357**, 1069–1071.
4 S. C. Szu, X. R. Li, A. L. Stone and J. B. Robbins, *Infect. Immun.*, 1991, **59**, 4555–4561.
5 K. L. O'Brien and M. Santosam, *Am. J. Epidemiol.*, 2004, **159**, 634–644.
6 (*a*) A. O. Tzianabos, A. B. Onderdonk, B. Rosner, R. L. Cisneros and D. L. Kasper, *Science*, 1993, **262**, 416–419; (*b*) A. O. Tzianabos, R. W. Finberg, Y. Wang, M. Chan, A. B. Onderdonk, H. J. Jennings and D. L. Kasper, *J. Biol. Chem.*, 2000, **275**, 6733–6740; (*c*) Y. Wang, W. M. Kalka-Moll, M. H. Roehrl and D. L. Kasper, *Proc. Natl. Acad. Sci. U. S. A.*, 2000, **97**, 13478–13483.
7 (*a*) Y.-H Choi, M. H. Roehrl, D. L. Kasper and J. Y. Wang, *Biochemistry*, 2002, **41**, 15144–15151; (*b*) A. O. Tzianabos, J. Y. Wang and J. C. Lee, *Proc. Natl. Acad. Sci. U. S. A.*, 2001, **98**, 9365–9370; (*c*) A. Tzianabos, J. Y. Wang and D. L. Kasper, *Carbohydr. Res.*, 2003, **338**, 2531–2538.
8 F. Y. Avci and D. L. Kasper, *Annu. Rev. Immunol.*, 2010, **28**, 107–110.
9 D. A. Case, T. A. Darden, T. E. Cheatham III, C. L. Simmerling, J. Wang, R. E. Duke, R. Luo, M. Crowley, R. C. Walker, W. Zhang, K. M. Merz, B. Wang, S. Hayik, A. Roitberg, G. Seabra, I. Kolossváry, K. F. Wong, F. Paesani, J. Vanicek, X. Wu, S. R. Brozell, T. Steinbrecher, H. Gohlke, L. Yang, C. Tan, J. Mongan, V. Hornak, G. Cui, D. H. Mathews, M. G. Seetin, C. Sagui, V. Babin and P. A. Kollman, 2008, *AMBER 10*, University of California, San Francisco.
10 J. Wang, R. M. Wolf, J. W. Caldwell, P. A. Kollamn and D. A. Case, *J. Comput. Chem.*, 2004, **25**, 1157–1174.
11 C. I. Bayly, P. Cieplak, W. D. Cornell and P. A. Kollman, *J. Phys. Chem.*, 1993, **97**, 10269–10280.
12 W. L. Jorgensen, J. Chandrasekhar, J. D. Madura, R. W. Impey and L. M. Klein, *J. Chem. Phys.*, 1983, **79**, 926–935.
13 J. P. Ryckaert, G. Ciccoti and H. J. C. Berendsen, *J. Comput. Phys.*, 1977, **23**, 327–341.
14 W. Humphrey, A. Dalke and K. Schulten, *J. Mol. Graphics*, 1996, **14**, 33–38.